

1 **Tao et al. (Supplementary Information)**

2 ***Pervasive correlation of molecular evolutionary rates in the tree of life***

3

4 **Machine learning model building**

5 **Training data.** We simulated nucleotide alignments using independent branch rate (IBR)
6 and correlated branch rate (CBR) models using the NELSI package¹. In IBR, branch-
7 specific rates were drawn from a lognormal distribution with a mean gene rate and a
8 standard deviation (in log-scale) that varied from 0.1 to 0.4, previously used in a study
9 simulating independent rates with different levels of variation¹. In CBR, branch-specific
10 rates were simulated under an autocorrelated process² with an initial rate set as the mean
11 rate derived from an empirical gene and an autocorrelated parameter, ν , that was
12 randomly chosen from 0.01 to 0.3, previously used in a study simulating low, moderate
13 and high degrees of autocorrelated rates¹. We used SeqGen³ to generate alignments
14 under Hasegawa-Kishino-Yano (HKY) model⁴ with 4 discrete gamma categories by using
15 a master phylogeny, consisting of 60-400 ingroup taxa randomly sampled from the bony-
16 vertebrate clade in the Timetree of Life⁵. Mean evolutionary rates, G+C contents,
17 transition/transversion ratios and numbers of sites for simulation were derived from
18 empirical distributions⁶. These 2,000 simulated datasets were used as training data in
19 building the machine learning model.

20 **Features acquisition.** Lineage-specific rate estimates (r_i 's) were obtained using
21 equations [28] - [31] and [34] - [39] in Tamura et al. (2018)⁷. As mentioned in the main
22 text, a lineage rate is a function of all the branch rates that belong to that lineage. For any
23 given node in the phylogeny, we extracted the relative rates of its ancestral clade (r_a) and
24 two direct descendant clades (r_1 and r_2). Then, we calculated correlation between
25 ancestral lineage and its direct descendant lineage rate to obtain estimates of ancestor-
26 descendant rate correlation (ρ_{ad}). We also calculated correlation between sister lineage
27 rates (ρ_s), for which the lineage rates of sister pairs are randomly labeled. The labeling of
28 sister pairs have small impact on ρ_s when the number of sequences in the phylogeny is
29 not too small (>50). However, one can also choose to resample sister pairs for multiple

30 times and use the mean of resampled ρ_s in the CorrTest in order to eliminate any bias
31 that may result from the arbitrary designation of sister rates during the correlation process,
32 which can be a problem when the number of taxa is small. To avoid the assumption of
33 linear correlation between lineages, we used Spearman rank correlation because it can
34 capture both linear and non-linear correlation between two vectors. Two additional
35 features derived from the relative rates in the phylogeny were used in building the
36 machine learning model. We first estimated ρ_{ad_skip1} as the correlation between rates
37 where the ancestor and descendant were separated by one intervening branch, and
38 ρ_{ad_skip2} as the correlation between rates where the ancestor and descendant were
39 separated by two intervening branches. This skipping reduces ancestor-descendant
40 correlation, which we then used to derive the decay of correlation values by using
41 equations $(\rho_{ad} - \rho_{ad_skip1})/\rho_{ad}$ and $(\rho_{ad} - \rho_{ad_skip2})/\rho_{ad}$. These two features improved the
42 accuracy of our model slightly. In the analyses of empirical datasets, we found that a large
43 amount of missing data (>50%) can result in unreliable estimates of branch lengths and
44 other phylogenetic errors⁸⁻¹². In this case, we recommend computing selected features
45 using only those lineage pairs for which >50% of the positions contain valid data, or
46 remove sequences with a large amount of missing data.

47 **Predictive model.** We trained a logistic regression model using the skit-learn module¹³,
48 which is a python toolbox for data mining and data analysis using machine learning
49 algorithms, with only ρ_{ad} , only ρ_s or all 4 features (ρ_s , ρ_{ad} , the two decay of correlation
50 features) using 2,000 simulated training datasets (1,000 with CBR model and 1,000 with
51 IBR model). A response value of 1 was given to true positive cases (correlated rates) and
52 0 was assigned to true negative cases (independent rates). Thus, the prediction scores
53 (CorrScore) were between 0 and 1. A high score representing a higher probability that
54 the rates are correlated. Then the global thresholds at 5% and 1% significant levels can
55 be determined. To explore the reliability of the global threshold, we re-trained the model
56 with all 4 features extracted from 4 subsets of training data with ≤ 100 (M100), 100 – 200
57 (M200), 200 – 300 (M300), and > 300 (M400) sequences. A specific threshold was
58 determined for each training subset and then was tested using Tamura *et al.* (2012)'s
59 data¹⁴ with the corresponding size. For example, we used the threshold determined by
60 the model trained with small data (≤ 100 sequences) on the test data that contain less

61 than 100 sequences, and used the threshold determined by the model trained with large
62 data (>300 sequences) on the large test data (400 sequences). We found that the
63 accuracy of using the specific thresholds (**Fig. S1a-c**) is similar to the accuracy when we
64 used a global threshold (**Fig. 3d-f**). This is because the machine learning algorithm has
65 automatically incorporated the impact of the number of sequences when it determined
66 the relationship of four selected features (ρ_{ad} , ρ_s , and 2 decays).

67 **Cross-validation**

68 We performed two cross-validation tests. In 10-fold cross-validation, the predictive model
69 was developed using 90% of the synthetic datasets, and then its performance was tested
70 on the remaining 10% of the datasets. The AUROC was greater than 0.99 and the
71 accuracy was high (>94%). Even in the 2-fold cross-validation, where only half of the
72 datasets were used for training the model and the remaining half were used for testing,
73 the AUROC was still greater than 0.99 with an accuracy greater than 92%. This indicates
74 that the features we used in building the machine learning model are powerful and
75 ensures high accuracy even when the training data are limited.

76 **External tests**

77 **Publicly available data.** Two previously published simulated dataset were used to
78 evaluate CorrTest's performance. Beaulieu et al.'s data¹⁵ contains 91 ingroup taxa with
79 1,000 base pairs each. For Tamura et al.'s data¹⁴, we present the test results for the data
80 simulated using CBR model (autocorrelated lognormal distribution) and IBR model
81 (independent uniform distribution with 50% rate variation) here. We tested the
82 performance of our model on CBR and IBR data with different GC contents,
83 transition/transversion ratios, and evolutionary rates. We randomly sampled 50, 100, 200,
84 and 300 sequences from the original 400 sequences and conducted CorrTest using the
85 correct, error-prone topology inferred by the Neighbor-joining method¹⁶ with an
86 oversimplified substitution model¹⁷. We also tested CorrTest's performance on data
87 simulated under an IBR model process with 100% rate variation and found that CorrTest
88 works perfectly (100% accuracy; results not shown).

89 **Synthetic data.** We conducted another set of simulations using IBR (independent
90 lognormal distribution) and CBR (autocorrelated lognormal distribution)² model with 100

91 replicates each using the same strategy as a training data simulation (described above)
92 on a master phylogeny of 100 taxa randomly sampled from the bony-vertebrate clade in
93 the Timetree of Life⁵. These 200 datasets were used to conduct CorrTest and Bayes
94 factor analyses and to obtain the autocorrelation parameter (ν) in MCMCTree¹⁸.

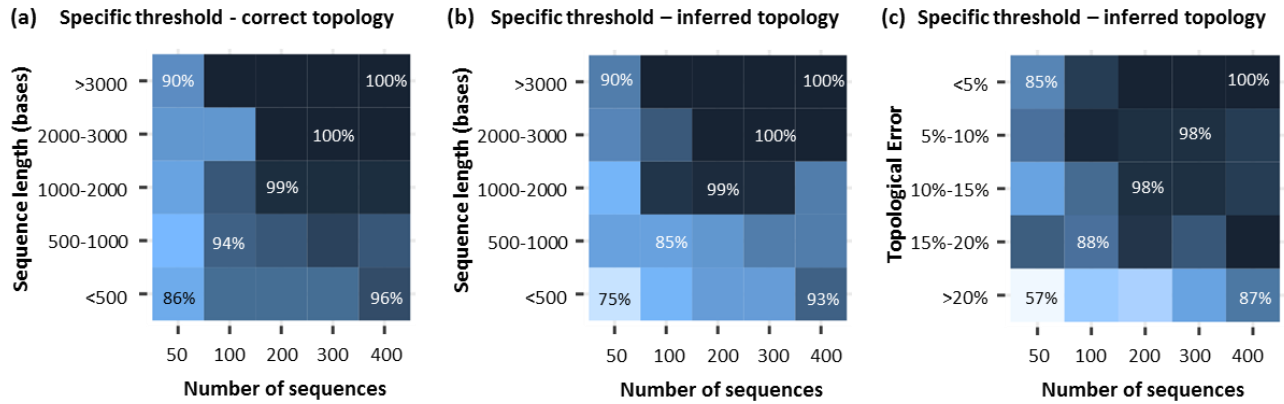
95

96 References

- 97 1. Ho, S. Y., Duchêne, S. & Duchêne, D. Simulating and detecting autocorrelation of
98 molecular evolutionary rates among lineages. *Mol. Ecol. Resour.* **15**, 688–696
99 (2015).
100
- 101 2. Kishino, H., Thorne, J. L. & Bruno, W. J. Performance of a divergence time
102 estimation method under a probabilistic model of rate evolution. *Mol. Biol. Evol.* **18**,
103 352–361 (2001).
104
- 105 3. Grassly, N. C., Adachi, J. & Rambaut, A. Seq-Gen: an application for the Monte
106 Carlo simulation of protein sequence evolution along phylogenetic trees. *Comput.*
107 *Appl. Biosci.* **13**, 235–238 (1997).
108
- 109 4. Hasegawa, M., Kishino, H. & Yano, T. Dating of the human-ape splitting by a
110 molecular clock of mitochondrial DNA. *J. Mol. Evol.* **22**, 160–174 (1985).
111
- 112 5. Hedges, S. B. & Kumar, S. *The Timetree of Life*. pp3–18 (New York: Oxford
113 University Press., 2009).
114
- 115 6. Rosenberg, M. S. & Kumar, S. Heterogeneity of nucleotide frequencies among
116 evolutionary lineages and phylogenetic inference. *Mol. Biol. Evol.* **20**, 610–621
117 (2003).
118
- 119 7. Tamura, K., Tao, Q. & Kumar, S. Theoretical foundation of the RelTime method for
120 estimating divergence times from variable evolutionary rates. *Mol. Biol. Evol.*
121 *msy044* (2018). doi:10.1093/molbev/msy044
122
- 123 8. Filipowski, A., Murillo, O., Freydenzon, A., Tamura, K. & Kumar, S. Prospects for
124 building large timetrees using molecular data with incomplete gene coverage among
125 species. *Mol. Biol. Evol.* **31**, 2542–2550 (2014).
126
- 127 9. Xi, Z., Liu, L. & Davis, C. C. The impact of missing data on species tree estimation.
128 *Mol. Biol. Evol.* **33**, 838–860 (2015).
129
- 130 10. Lemmon, A. R., Brown, J. M., Stanger-Hall, K. & Lemmon, E. M. The effect of
131 ambiguous data on phylogenetic estimates obtained by maximum likelihood and
132 Bayesian inference. *Syst. Biol.* **58**, 130–145 (2009).
133

- 134 11. Wiens, J. J. & Moen, D. S. Missing data and the accuracy of Bayesian
135 phylogenetics. *Journal of Systematics and Evolution* **46**, 307–314 (2008).
136
- 137 12. Marin, J. & Hedges, S. B. Undersampling genomes has biased time and rate
138 estimates throughout the tree of life. *Mol. Biol. Evol.* msy103 (2018).
139 doi:doi.org/10.1093/molbev/msy103
140
- 141 13. Pedregosa, F. *et al.* Scikit-learn: Machine learning in Python. *J. Mach. Learn. Res.*
142 **12**, 2825–2830 (2011).
143
- 144 14. Tamura, K. *et al.* Estimating divergence times in large molecular phylogenies. *Proc.*
145 *Natl. Acad. Sci. U.S.A.* **109**, 19333–19338 (2012).
146
- 147 15. Beaulieu, J. M., O'Meara, B. C., Crane, P. & Donoghue, M. J. Heterogeneous rates
148 of molecular evolution and diversification could explain the Triassic age estimate for
149 angiosperms. *Syst. Biol.* **64**, 869–878 (2015).
150
- 151 16. Saitou, N. & Nei, M. The neighbor-joining method: a new method for reconstructing
152 phylogenetic trees. *Mol. Biol. Evol.* **4**, 406–425 (1987).
153
- 154 17. Kimura, M. A simple method for estimating evolutionary rates of base substitutions
155 through comparative studies of nucleotide sequences. *J. Mol. Evol.* **16**, 111–120
156 (1980).
157
- 158 18. Yang, Z. PAML 4: phylogenetic analysis by maximum likelihood. *Mol. Biol. Evol.* **24**,
159 1586–1591 (2007).

160



161

162

163 **Figure S1.** Patterns of CorrTest accuracy using M100, M200, M300, and M400 models
164 for the corresponding test datasets¹⁴. Accuracies are shown for increasing number of
165 sequences. The accuracy of CorrTest for different sequence length is shown when (a)
166 the correct topology was assumed and (b) the topology was inferred. (c) The accuracy of
167 CorrTest for datasets in which the inferred the topology contained small and large number
168 of topological errors.

169

170